SciencePG
Science Publishing Group

Physicochemical Characterization of Biofield Treated Orchid Maintenance/Replate Medium

Mahendra Kumar Trivedi[1], Alice Branton[1], Dahryn Trivedi[1], Gopal Nayak[1], Ragini Singh[2], Snehasis Jana[2, *]

[1]Trivedi Global Inc., Henderson, NV, USA
[2]Trivedi Science Research Laboratory Pvt. Ltd., Bhopal, Madhya Pradesh, India

Email address:

publication@trivedisrl.com (S. Jana)

Abstract: Orchids are used worldwide for indoor decoration, vanilla production, and beverage preparation. They are also reported for their therapeutic efficacy in brain-related problems. The *in vitro* micropropagation technique was used for their propagation using the orchid maintenance/replate (OMR) medium. The current study was based on analysing the effect of biofield energy treatment on the physicochemical properties of OMR medium. A part of the sample was treated with Mr. Trivedi's biofield energy; various physicochemical properties were analyzed and compared with the untreated (control) part. The X-ray diffraction analysis revealed the decrease in crystallite size of treated sample (132.80 nm) as compared to the control (147.55 nm). The particle size analysis revealed 20.78% increase in average particle size and 39.29% increase in d_{99} (size below which 99% particles are present) of the treated OMR medium as compared to the control. Moreover, the surface area of the treated sample was reduced by 3.9%, supporting the data of particle size analysis. The thermal analysis studies revealed an increase in the thermal stability of the treated OMR medium as compared to the control. The analysis was done by using differential scanning calorimetry that showed increase in melting point (1.23%) and latent heat of fusion (135.7%); and thermogravimetric analysis that reported increase in onset temperature and maximum thermal degradation temperature of the treated sample as compared to the control. Besides, the CHNSO analysis revealed the increase in percentage of nitrogen (22.22%) as well as the presence of sulphur in the treated sample. The Fourier transform infrared and UV-visible spectroscopy also showed the differences in the spectra of the treated sample as compared to the control OMR medium. Hence, the overall data revealed the impact of biofield energy treatment on the physicochemical properties of the treated sample that might be used in better way in the *in vitro* culture techniques as compared to the control sample.

Keywords: Orchid Maintenance/Replate Medium, Biofield Energy Treatment, *In vitro* Micropropagation, Complementary and Alternative Medicines

1. Introduction

Orchids belonging to family *Orchidaceae* are widely used due to their medicinal properties in several countries around the world [1]. Several kind of research had shown their therapeutic efficacy in case of hysteria, nervous irritability, and other brain related dysfunctions. Besides, several species are reported as a febrifuge, clearing tapeworms, treating skin diseases, *etc.* [2, 3]. It was reported that the biological activity was due to the presence of alkaloids such as strychnine, morphine, nicotine, reserpine, *etc.* [4]. Moreover, the orchid family is also important for its horticulture uses. It is used for commercial production of vanilla [5]. In Turkey, it is used in the preparation of a traditional beverage called as salep [3]. It has great importance as cut flowers and indoor decoration. The general method of propagation of orchid is asexual but it can produce only 2-4 plants per year as it is very slow process [6, 7]. Hence, *in vitro* micropropagation technique is frequently used that produces plantlets using tissue culture techniques [8]. Micropropagation is the process used to replicate the plant using plant seed or tissue in the laboratory under the sterile conditions [9]. The most important factor in successful tissue culture of plant cells is

the composition of the medium. It provides the essential nutrients for the survival of plant cells or tissues and the optimum conditions such as pH, osmotic pressure, *etc*. [10]. Orchid maintenance/replate (OMR) medium is such type of medium that consists of accurately defined organic and inorganic chemical additives in the form of macro- and micronutrients [11]. The constituents of the medium are shown in Table 1. It differs from original orchid replate medium as it contains banana powder to promote rooting and growth, and agar as a gelling agent that provides physical support [12]. Despite several advantages, it suffers the problem of hygroscopicity due to which it needs to be protected from atmospheric moisture and proper storage conditions (2-8°C) [13]. Hence, some alternative is needed that can improve its properties thereby its use as orchid micropropagation medium.

Table 1. Components of the orchid maintenance/replate medium.

S. No.	Ingredient	milligram/litre
1	Potassium nitrate	950.00
2	Ammonium nitrate	825.00
3	Calcium chloride.2H$_2$O	220.00
4	Magnesium sulphate	90.34
5	Potassium phosphate monobasic	85.00
6	Manganese sulphate.H$_2$O	8.45
7	Boric acid	3.10
8	Potassium iodide	0.42
9	Molybdic acid (sodium salt).2H$_2$O	0.13
10	Zinc sulphate.7H$_2$O	5.30
11	Copper sulphate.5H$_2$O	0.0125
12	Cobalt chloride.6H$_2$O	0.0125
13	Ferrous sulphate.7H$_2$O	27.80
14	EDTA disodium salt.2H$_2$O	37.30
15	myo - Inositol	100.00
16	Thiamine hydrochloride	10.00
17	Pyridoxine hydrochloride	1.00
18	Nicotinic acid (Free acid)	1.00
19	Peptone	2000.00
20	Banana powder	30000.00
21	Sucrose	20000.00
22	MES	1000.00
23	Agar	7000.00
24	Activated charcoal	2000.00

MES: 2-(n-morpholino)ethanesulfonic acid; EDTA: Ethylenediamine tetraacetic acid

The biofield energy treatment is reported to affect the health of human beings *via* interacting with their biofield [14]. The National Centre for Complementary and Alternative Medicine (NCCAM), which is the part of National Institute of Health (NIH) also include the energy medicines as complementary and alternative medicines (CAM) [15]. It is a putative form of energy that is produced by own emissions of the body and surrounds the body of all living organisms. However, the frequency of this energy depends on the physiological and mental state of the person. The living systems are continuously exchanging this energy with their surroundings to maintain themselves [16, 17]. The non-living things also possess the biofield energy as everything in the universe made up of same constituents; however, they are not able to change their energy aura by

more than 2% [18]. Thus, the human has the ability to harness the energy from the environment and can transmit it to any living or non-living object. Mr. Trivedi is also known to possess unique biofield energy, and the treatment is called as The Trivedi Effect®. It is known for its impact on various living organisms and non-living materials including microorganisms [19], pharmaceutical compounds [20], and yield, growth, and anatomical characteristics of plants [21, 22]. Hence, based on the importance of OMR medium and the outcomes of the biofield energy treatment, the study was designed to analyse the impact of Mr. Trivedi's biofield energy treatment on various physicochemical properties of the OMR medium.

2. Materials and Methods

Orchid maintenance/replate (OMR) Medium was procured from HiMedia Laboratories, India. The sample was divided into two parts and coded as control and treated. Mr. Trivedi's biofield energy treatment was provided to the treated part while no treatment was given to the control part. For treatment, the treated part was handed over to Mr. Trivedi in sealed pack under standard laboratory conditions. Mr. Trivedi provided the treatment to the treated part through his unique energy transmission process, without touching the sample. The control and biofield treated samples were further characterised using various analytical techniques.

2.1. X-ray Diffraction (XRD) Study

The Phillips Holland PW 1710 X-ray diffractometer system was used to obtain the X-ray powder diffractogram of control and treated samples. The X-ray generator was equipped with a copper anode with nickel filter operating at 35kV and 20mA. The XRD system used 1.54056Å wavelength of radiation. The data were collected from the 2θ range of 10°-99.99° and a counting time of 0.5 seconds per step along with a step size of 0.02°.

The crystallite size (G) was calculated from the Scherrer equation:

$$G = k\lambda/(bCos\theta)$$

Where, k is constant (0.94), λ is the X-ray wavelength (0.154 nm), b in radians is the full-width at half of the peak and θ is the corresponding Bragg's angle.

Moreover, the percent change in crystallite size was calculated using the following equation:

$$\text{Percent change in crystallite size} = [(G_t-G_c)/G_c] \times 100$$

Here, G_c and G_t denotes the crystallite size of control and treated powder samples, respectively.

2.2. Particle Size Analysis

For particle size analysis, laser particle size analyzer SYMPATEC HELOS-BF was used, having a detection range of 0·1-875 μm. Two parameters of particle sizes *viz*. d_{50} and d_{99} (size below which 50% and 99% particles are

present, respectively) were calculated. The percent change in average particle size (d_{50}) was calculated using following equation:

$$\% \text{ change in particle size, } d_{50} = \frac{[(d_{50})_{\text{Treated}} - (d_{50})_{\text{Control}}]}{(d_{50})_{\text{Control}}} \times 100$$

Where, $(d_{50})_{\text{Control}}$ and $(d_{50})_{\text{Treated}}$ represents the average particle size of control and treated samples, respectively. Similarly, the percent change in particle size d_{99} was calculated.

2.3. Surface Area Analysis

The surface area was measured by the Brunauer–Emmett–Teller (BET) surface area analyser, Smart SORB 90. The percent change in surface area was calculated using following equation:

$$\% \text{ change in surface area } = \frac{[S_{\text{Treated}} - S_{\text{Control}}]}{S_{\text{Control}}} \times 100$$

Where, S_{Control} and S_{Treated} are the surface area of control and treated samples respectively.

2.4. Thermal Analysis

The thermal stability profile of OMR medium was analyzed using DSC and TGA/DTG studies. The impact of biofield treatment was analyzed by comparing the results of treated sample with that of the control sample.

2.4.1. Differential Scanning Calorimetry (DSC) Study

The DSC analysis of control and treated samples was carried out using Perkin Elmer/Pyris-1. The samples were heated at a rate of 10°C/min under air atmosphere (5 mL/min). The thermograms were collected over the temperature range of 50°C to 300°C.

2.4.2. Thermogravimetric Analysis/Derivative Thermogravimetry (TGA/DTG)

The effect of temperature on the stability of the control and treated sample of OMR medium was analyzed using Mettler Toledo simultaneous thermogravimetric analyser (TGA/DTG). The heating temperature was selected from room temperature to 350°C with a heating rate of 5°C/min under air atmosphere.

2.5. CHNSO Analysis

The control and treated samples of OMR medium were analyzed using CHNSO analyzer using Model Flash EA 1112 series, Thermo Finnigan Italy.

2.6. Fourier Transform-Infrared (FT-IR) Spectroscopic Characterization

For FT-IR characterization, the samples were crushed, mixed with spectroscopic grade KBr and pressed into pellets with a hydraulic press. The FT-IR spectra were recorded on Shimadzu's Fourier transform infrared spectrometer (Japan) in the frequency range 4000-350 cm^{-1}. The FT-IR spectral analysis was used to determine the effect of biofield energy on the strength of bonds and stability of compounds present in OMR medium.

2.7. UV-Vis Spectroscopic Analysis

The UV-Vis spectral analysis was measured using Shimadzu UV-2400 PC series spectrophotometer. The spectrum was recorded using 1 cm quartz cell that has a slit width of 2.0 nm.

3. Results and Discussion

3.1. X-Ray Diffraction (XRD)

The X-ray powder diffractograms of control and treated samples of OMR medium showed a series of sharp peaks in the regions of 10º<2θ>40º. In the control sample, the peaks were observed at 2θ equal to 11.67°, 16.72°, 18.72°, 18.88°, 19.64°, 21.49°, and 25.23°. However, the treated sample showed the peaks at 2θ equal to 11.61°, 13.05°, 16.67°, 17.73°, 18.74°, 22.04°, 24.64°, and 25.17°. In addition, the most intense peak in control sample was observed at 2θ equal to 25.23°; however, in treated sample it was observed at 22.04°. It indicated that the relative intensities of XRD peaks were altered in the treated OMR medium as compared to the control sample. Besides, the crystallite size of the control sample was found as 147.55 nm whereas; in the treated sample it was found as 132.80 nm. It suggested that crystallite size of the treated sample was significantly decreased by 10% as compared to the control. The changes in the relative intensities of peaks revealed the presence of microstrain may be due to the biofield treatment. It may result in change in dislocation densities and atomic displacements that might be the reason for decreased crystallite size [23, 24].

3.2. Particle Size Analysis

The particle size of control and treated samples of OMR medium are presented in Fig. 1. It showed that the d_{50} and d_{99} were 26.03 and 236.92 μm, respectively in the control sample. However, in treated sample, the d_{50} and d_{99} were found as 31.44 and 330.01 μm, respectively. It revealed that d_{50} was increased by 20.78% and d_{99} was increased by 39.29% in the treated sample as compared to the control. The temperature has a significant effect on the particle size of the sample [25]. Hence, it is presumed that the biofield treatment may provide some energy to the sample that resulted in increased particle size as compared to the control sample. Moreover, the particle size was directly related to the viscosity and gelling property of the compound [26]. Hence, the treated OMR medium sample with increased particle size might improve the gelling property of media, as the large particles has less tendency to broken down and has stronger water holding capacity as compared with the small particles.
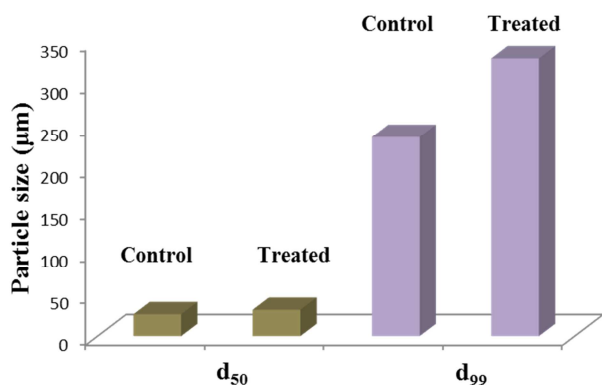
Fig. 1. *Particle size analysis of control and treated samples of OMR medium.*

3.3. Surface Area Analysis

The surface area of control and treated samples of OMR

medium was investigated using BET method. The control sample showed a surface area of 2.327 m^2/g; however, the treated sample of OMR medium showed a surface area of 2.236 m^2/g. It showed that the surface area was decreased by 3.91% in the treated OMR medium sample as compared to the control. The decrease in surface area of treated OMR medium sample may be due to the increase in the particle size as evident from the particle size analysis. Besides, the OMR medium has the problem of hygroscopicity [13] and the surface area was directly related to the hygroscopic water content of the sample [27]. Hence, it is assumed that the treated OMR medium sample with decreased surface area might reduce the problem of hygroscopicity as compared with the control sample.
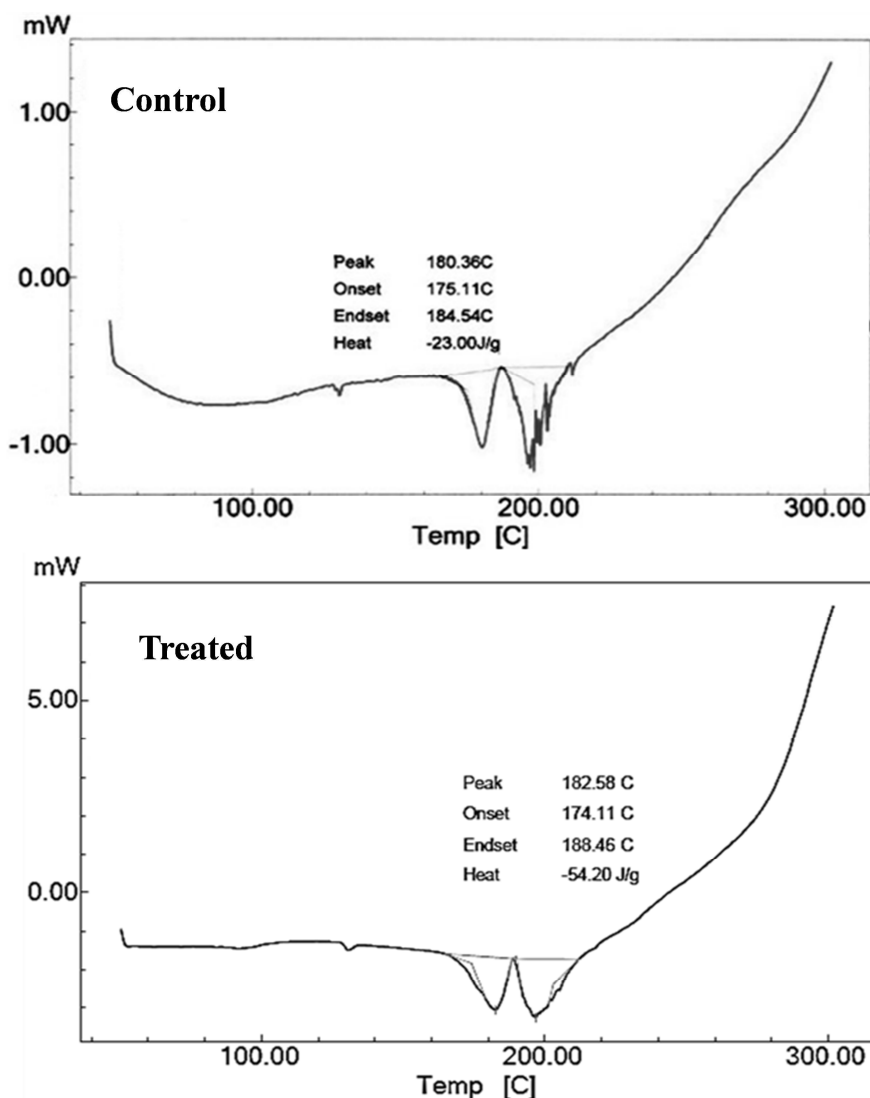
3.4. Thermal Analysis

3.4.1. DSC Analysis

Fig. 2. *DSC analysis of control and treated samples of OMR medium.*

The DSC thermograms of control and treated samples of OMR medium are presented in Fig. 2. The thermogram of control sample showed an endothermic peak at 180.36°C due to the melting of the sample. In this process, the amount of heat absorbed (latent heat of fusion, ΔH) was recorded as 23.00 J/g. The similar endothermic peak was observed in

treated sample at 182.58°C and ΔH was recorded as 54.20 J/g. The result of DSC analysis revealed slight alteration (1.23% increase) in the melting temperature along with 135.7% increase in ΔH. The particle size can influence the melting temperature and ΔH of the corresponding sample as it is directly related to the melting properties [28, 29]. Hence, it might be a reason for the increase in melting temperature and ΔH of the OMR medium as the particle size was found increased after the biofield treatment.

3.4.2. TGA/DTG Analysis

The TGA/DTG studies analyse the pattern of thermal decomposition of the sample during heating. The TGA/DTG thermograms of the control and treated samples of OMR medium are presented in Fig. 3. The thermogram of control sample showed the degradation of the sample in three steps. Moreover, the first step degradation of the sample was started at 175.72°C and ended at 203.38°C. Besides, the treated sample showed two-step degradation, where the first step commenced at 187.61°C and completed at 237.96°C. It indicated that the onset temperature of degradation was

increased in the treated sample as compared to the control. Besides, DTG thermogram data showed that T_{max} was observed at 189.19°C in the control sample while 210.41°C in the treated OMR medium. It indicated that T_{max} was increased by approximately 21°C in the treated sample as compared to the control. Furthermore, the increase in onset temperature of decomposition and T_{max} in the treated sample of OMR medium with respect to the control sample may be correlated with the increased thermal stability. The particle size has a significant impact on the onset and peak temperature and they were found directly proportional to each other [29]. Hence, the increase in particle size of OMR medium after treatment might be a reason for the increase in thermal stability. Besides, it is well known that the OMR medium faces high-temperature treatment (*e.g.,* autoclaving) before used as culture media where it may suffer from the problem of thermal degradation. Hence, the treated sample with increased thermal stability might help in increasing the efficacy and shelf-life of the treated sample as compared to the control.
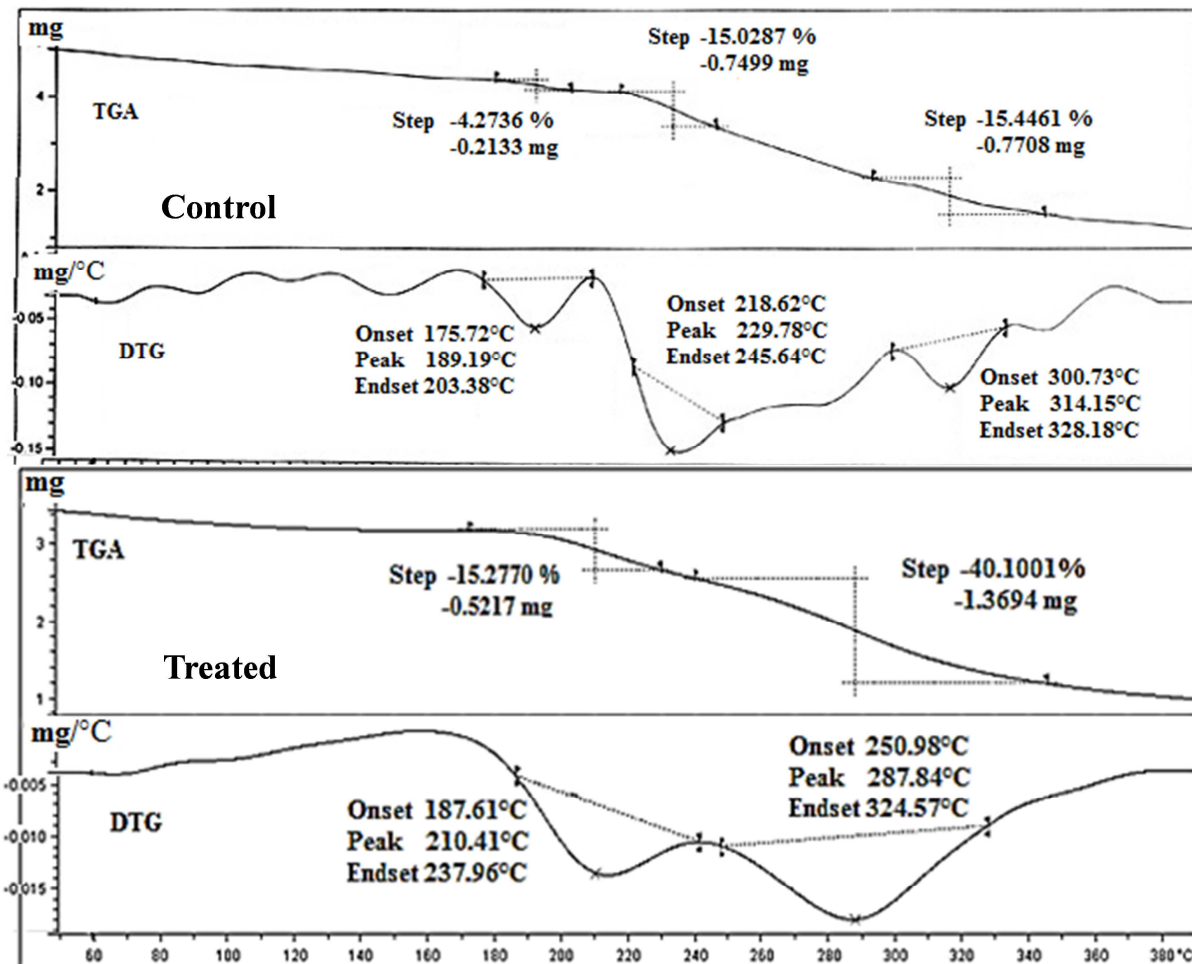

Fig. 3. *TGA/DTG analysis of control and treated samples of OMR medium.*

3.5. CHNSO Analysis

The CHNSO analysis was used to measure the percentage

of elements present in the given sample. The result of CHNSO analysis of control and treated samples are presented in Table 2. The data revealed that the percentage of nitrogen was significantly increased by 22.22% whereas; the

percentage of carbon, hydrogen, and oxygen was slightly decreased as 3.62, 8.51, and 1.92%, respectively in the treated sample as compared to the control. Besides, the treated sample showed the presence of sulphur that was not detected in the control sample. It is well known that nitrogen is the main component of media that is provided by ammonium nitrate, potassium nitrate, and peptone. The increased percentage of nitrogen in the treated sample may help to improve the growth of orchid culture as compared with the control.

Table 2. CHNSO data of orchid maintenance / replate medium.

Element	Control	Treated	Percent change
Nitrogen	0.63	0.77	22.22
Carbon	43.90	42.31	-3.62
Hydrogen	6.93	6.34	-8.51
Oxygen	31.18	30.58	-1.92
Sulphur	ND	0.27	

ND: not detected

3.6. FT-IR Spectroscopic Analysis
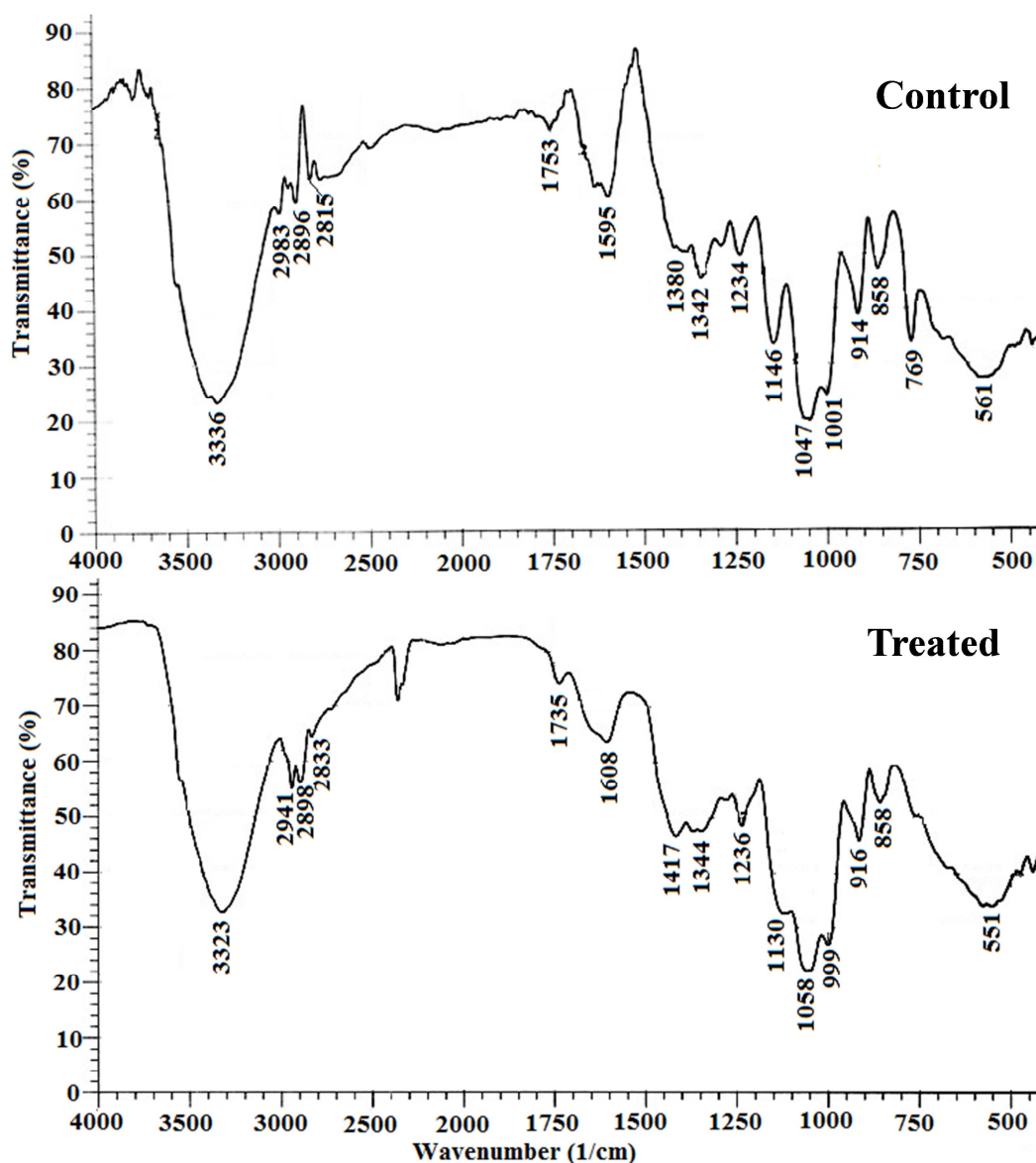
Fig. 4. FT-IR spectra of control and treated samples of OMR medium.

The FT-IR spectra of OMR medium (control and treated samples) are shown in Fig. 4. The sample contains several ingredients such as ammonium nitrate, disodium EDTA, ferrous sulphate, potassium nitrate, nicotinic acid, sucrose, inositol, thiamine hydrochloride, and pyridoxine hydrochloride, *etc*. Hence, the major vibration peaks were observed (Table 3) related to the functional groups present in these ingredients. The peak at 3336 cm^{-1} in the control

sample was assigned to N-H stretching of ammonium nitrate and O-H stretching (carboxylic acid) due to nicotinic acid and disodium EDTA [30] [31]; however, the broadness of peak suggests the hydrogen bonding within the compound. Besides, in the treated sample it was shifted to a lower frequency at 3323 cm^{-1}. Further, the C-H stretching peaks of disodium EDTA appeared at 2983 and 2896 cm^{-1} in the control sample, whereas, in the treated sample, the peaks

appeared at 2941 and 2898 cm^{-1}. The peak due to pyridine ring of nicotinic acid and pyridoxine HCl was observed at 2815 cm^{-1} in the control, while 2833 cm^{-1} in the treated sample. Similarly, the peak at 1753 cm^{-1} in the control sample was assigned to C=O stretching of lactone ring present in sucrose; however, it was observed at 1735 cm^{-1} in the treated sample [30]. The peak at 1595 cm^{-1} in the control sample appeared as doublet and it was assigned to ring stretching of the pyridine ring of nicotinic acid and pyridoxine HCl [32]. The peak may also merge with the peak due to S-O bond of CuSO$_4$ and P-O bond of KPO$_4$ [31]. Besides, in the treated sample the corresponding peak was observed as a singlet at 1608 cm^{-1}. Furthermore, the peak at 1380 cm^{-1} in the control that was shifted to 1417 cm^{-1} in the treated sample was assigned to N-O symmetric stretching of KNO$_3$ and pyrimidine ring of thiamine HCl [31, 32]. The peaks at 1234 cm^{-1} in the control sample and 1236 cm^{-1} in the treated sample was assigned to thiazole ring breathing of the thiamine HCl [33]. Moreover, the peak at 1146 and 1130 cm^{-1} in the control and treated samples, respectively was assigned to S-O bond in FeSO$_4$ and ZnSO$_4$, and pyrimidine ring of thiamine HCl. The peak due to C-O stretching of alcohol group in pyridoxine HCl was observed at 1047 cm^{-1} in the control and 1058 cm^{-1} in the treated sample. The ring breathing mode of inositol was observed at 1001 cm^{-1} in the control and 999 cm^{-1} in the treated sample. Further, the peak at 858 cm^{-1} in both, control and treated sample was assigned to B-O bond of boric acid and C-H out of plane bending of thiazole ring in thiamine HCl. The IR peaks of control sample were well matched with the reported literature. The FT-IR spectra of the treated sample showed different IR frequencies of respective functional groups as compared to the control. It suggested the impact of biofield energy treatment on the bond strength and dipole moment of the compounds present in the OMR medium. However, further studies are needed to analyse the effect of this treatment on the specific compounds and their functions in OMR medium.

Table 3. Vibration modes observed in orchid maintenance/replate medium.

S. No.	Functional group	Compound	Wavenumber (cm^{-1})	
			Control	Treated
1	O-H stretching, N-H stretching	Nicotinic acid, Disodium EDTA Ammonium nitrate	3336	3323
2	C-H stretching	Disodium EDTA, Thiamine HCl	2983, 2896	2941, 2898
3	C-H stretching	Agar	2815	2833
4	C=O stretching (lactone)	Sucrose	1753	1735
5	Ring stretching (pyridine)	Nicotinic acid, Pyridoxine HCl	1595	1608
6	N-O stretching, Ring stretching (pyrimidine)	KNO$_3$, Thiamine HCl	1380	1417
7	Ring breathing (thiazole), S=O stretching	Thiamine HCl MES	1234	1236
8	Pyrimidine ring stretching, S-O bond	Thiamine HCl, FeSO$_4$, ZnSO$_4$	1146	1130
9	C-O stretching (C-OH)	Pyridoxine HCl	1047	1058
10	Ring breathing (carbon ring)	Inositol	1001	999
11	B-O stretching	Boric acid	858	858
12	Ring deformation (cycloalkane)	Inositol	561	551

3.7. UV-Vis Spectroscopic Analysis

The UV spectra of OMR medium (control and treated samples) are shown in Fig. 5. The UV spectrum of control sample showed absorption peaks at λ_{max} equal to 212 and 257 nm. However, the biofield treated sample showed absorption peaks at λ_{max} equal to 212 and 275 nm. The peak at λ_{max} 257 nm in the control sample was shifted to higher wavelength *i.e.* 275 nm in the treated sample. It is hypothesized that biofield energy treatment might affect the HOMO→LUMO transition within the compounds of OMR medium due to which the peak at λ_{max} 257 nm was shifted to 275 nm in the treated sample.
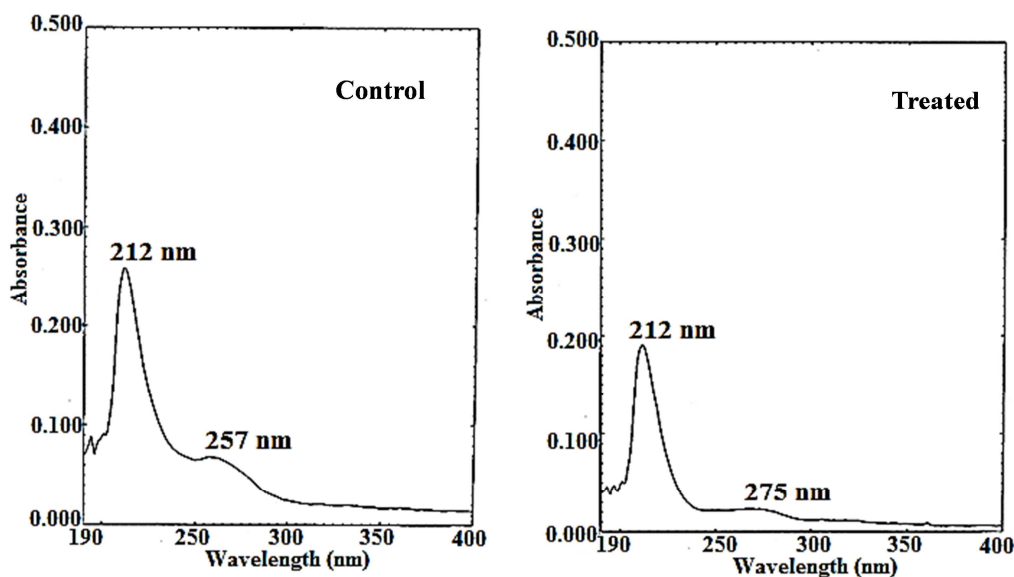
Fig. 5. UV-Vis spectra of control and treated samples of OMR medium.

4. Conclusions

The XRD study showed 10% decrease in the crystallite size of treated sample along with alteration in the relative intensities of the peaks. It may occur due to the presence of microstrains that might be generated after biofield energy treatment. Moreover, the average particle size and d_{99} were increased in treated sample by 20.78% and 39.29%, respectively as compared to the control. The surface area data supported the results of particle size analysis and revealed that the surface area was decreased by 4% in the treated sample. The increased particle size and reduced surface area might improve the gelling properties and reduce the problem of hygroscopicity of the treated sample. Besides, the melting temperature and ΔH was found increased in the treated sample as compared to the control. The TGA results also revealed that the onset temperature of degradation and maximum degradation temperature was increased in the treated sample. The increased thermal stability may help in increasing the efficacy and shelf-life of the treated sample as compared to the control. Furthermore, the CHNSO analysis revealed increased percent of nitrogen along with the presence of sulphur in the treated sample as compared to the control. The FT-IR and UV-vis spectra of the treated sample also revealed the changes as compared to the control. The overall study revealed the impact of biofield treatment on the physical, thermal and spectroscopic properties of the OMR medium that could make it more useful as compared to the control.

Acknowledgements

References

[1] Atwood JT (1986) The size of the orchidaceae and systematic position of epiphytic orchids. Selbyana 9: 171-186.

[2] Jalal JS, Kumar P, Tewari L, Pangtey YPS. Orchids: Uses in traditional medicine in India. National seminar on medicinal plants of Himalaya: Potential and prospect. Regional Research Institute of Himalayan Flora, Tarikhet, India.

[3] Bulpitt CJ (2005) The uses and misuses of orchids in medicine. QJM 98: 625-631.

[4] Bulpitt CJ, Li Y, Bulpitt PF, Wang J (2007) The use of orchids in chinese medicine. J R Soc Med 100: 558-563.

[5] Sforza S (2013) Food authentication using bioorganic molecules. DEStech Publications, Inc. USA.

[6] Khatun H, Khatun MM, Biswas MS, Kabir MR, Al-Amin M (2010) *In-vitro* growth and development of *Dendrobium hybrid* orchid. Bangladesh J Agr Res 35: 507-514.

[7] Nasiruddin KM, Begum R, Yasmin S (2003) Protocorm like bodies and plantlet regeneration from *Dendrobium formosum* leaf callus. Asian J Plant Sci 2: 955-957.

[8] Parvin MS, Haque ME, Akhter F, Moniruzzaman, Khaldun ABM (2009) Effect of different levels of naa on *in vitro* growth and development of shoots of *Dendrobium* orchid. Bangladesh J Agr Res 34: 411-416.

[9] Leva A, Rinaldi LMR (2012) Recent advances in plant *in vitro* culture. In Tech.

[10] Saad AIM, Elshahed AM. Plant tissue culture media. InTech

[11] Murashige T, Skoog F (1962) A revised medium for rapid growth and bioassays with tobacco tissue cultures. Physiol Plant 15: 473-497.

[12] Mazumder PB, Sharma GD, Choudhury MD, Nath D, Talukdar AD, et al. (2010) *In vitro* propagation and phytochemical screening of *Papilionanthe teres* (Roxb.) Schltr. Assam university journal of science & technology: Biological and environmental sciences 5: 37-42.

[13] http://www.funakoshi.co.jp/data/datasheet/PHT/O799.pdf

[14] Garland SN, Valentine D, Desai K, Li S, Langer C, et al. (2013) Complementary and alternative medicine use and benefit finding among cancer patients. J Altern Complement Med 19: 876-881.

[15] NIH, National Center for Complementary and Alternative Medicine. CAM Basics. Publication 347. [October 2, 2008]. Available at: http://nccam.nih.gov/health/whatiscam/

[16] Saad M, Medeiros RD (2012) Distant healing by the supposed vital energy- scientific bases. Complementary therapies for the contemporary healthcare. InTech.

[17] Rubik B (2002) The biofield hypothesis: Its biophysical basis and role in medicine. J Altern Complement Med 8: 703-717.

[18] Prakash S, Chowdhury AR, Gupta A (2015) Monitoring the human health by measuring the biofield "aura": An overview. IJAER 10: 27654-27658.

[19] Trivedi MK, Patil S, Shettigar H, Gangwar M, Jana S (2015) Antimicrobial sensitivity pattern of *Pseudomonas fluorescens* after biofield treatment. J Infect Dis Ther 3: 222.

[20] Trivedi MK, Patil S, Shettigar H, Singh R, Jana S, et al. (2015) An impact of biofield treatment on spectroscopic characterization of pharmaceutical compounds. Mod Chem appl 3:159.

[21] Sances F, Flora E, Patil S, Spence A, Shinde V (2013) Impact of biofield treatment on ginseng and organic blueberry yield. Agrivita J Agric Sci 35: 22-29.

[22] Patil SA, Nayak GB, Barve SS, Tembe RP, Khan RR (2012) Impact of biofield treatment on growth and anatomical characteristics of *Pogostemon cablin* (Benth.). Biotechnology 11: 154-162.

[23] Zhang K, Alexandrov IV, Kilmametov AR, Valiev RZ, Lu K (1997) The crystallite-size dependence of structural parameters in pure ultrafine-grained copper. J Phys D Appl Phys 30: 3008-3015.

[24] Trivedi MK, Tallapragada RR (2008) A transcendental to changing metal powder characteristics. Met Powder Rep 63: 22-28.

[25] Qu Y, Yang H, Yang N, Fan Y, Zhu H, et al. (2006) The effect of reaction temperature on the particle size, structure and magnetic properties of coprecipitated $CoFe_2O_4$ nanoparticles. Mater Lett 60: 3548-3552.

[26] Sun Q, Wu M, Bu X, Xiong L (2015) Effect of the amount and particle size of wheat fiber on the physicochemical properties and gel morphology of starches. PLoS One 10: e0128665.

[27] Amer AM (2009) Moisture adsorption capacity and surface area as deduced from vapour pressure isotherms in relation to hygroscopic water of soils. Biologia 64: 516-521.

[28] Levitas VI, Pantoya ML, Chauhan G, Rivero I (2009) Effect of the alumina shell on the melting temperature depression for aluminum nanoparticles. J Phys Chem C Nanomater Interfaces 113: 14088-14096.

[29] Martinez E (1961) The effect of particle size on the thermal properties of serpentine minerals. Am Mineral 46: 901-912.

[30] Lambert JB (1987) Introduction to organic spectroscopy. Macmillan, New York, USA.

[31] Miller FA, Wilkins CH (1952) Infrared spectra and characteristic frequencies of inorganic ions: Their use in qualitative analysis. Analytical Chemistry 24: 1253-1294.

[32] Breda S, Reva ID, Lapinski L, Nowak MJ, Fausto R (2006) Infrared spectra of pyrazine, pyrimidine and pyridazine in solid argon. J Mol Struct 786: 193-206.

[33] Rao CNR, Venkataraghavan R (1964) Contribution to the infrared spectra of five-membered N- and N, S-heterocyclic compounds. Can J Chem 42: 43-49.